Chapter VII

Phase Transitions and Near-Critical Phenomena

D. Beysens*, J. Straub**, D.J. Turner***

Gravity on earth limits the study of the gas-liquid critical point of pure fluids: the compressibility diverges, the fluid becomes stratified under its own weight and a bulk sample at its critical point cannot be obtained. Heating and cooling of near-critical fluids causes severe and prolonged convective instabilities as a consequence of the divergence of the expansibility. Studies on phase separation processes are similarly affected by convection and sedimentation.

A number of experimental investigations have taken advantage of the availability of a microgravity environment to overcome these limitations.They are reviewed in this paper and future prospects are assessed. Microgravity studies having the following objectives are justifiable: (i) testing of theoretical predictions and resolving discrepancies between predictions and experiment; (ii) understanding the mechanisms which precede the attainment of equilibrium near the critical point; (iii) evidencing the processes during phase separations when gravity-driven instabilities are eliminated; (iv) understanding the interfacial phenomena in reduced gravity and (v) understanding the physical chemistry of electrolyte solutions in compressible solvents.

A. Introduction

One of the most fundamental phase transitions is that between the vapour and the liquid phase of a pure fluid. Towards the end of the last century van der Waals [1] made use of the extensive studies of Andrews [2] and provided his classical explanation of the influence of temperature and pressure on a fluid's density. He subsequently showed that, when temperatures and pressures are appropriately scaled, all fluids behave in a similar manner [3]. This is called the Principle of Corresponding States. The reference point, from which all fluid transition properties can be derived, is the critical point: the point (characterized by one fixed temperature, pressure and density) at which the distinction between the gas and the liquid phase just disappears.

At the critical point, the compressibility of the fluid is infinite and close to it, it is very large. As a consequence, the fluid stratifies under its own weight so that any measurements made in a cell of finite height will actually measure an averaged property of the fluid at different densities rather than the real property at the critical point. This fundamental limitation imposed by the earth's gravity on experiments in the near-critical region was first conclusively demonstrated by Gouy in 1892 [4]. For a pure fluid, gravity effects are large only very close

* Centre d'Etudes Nucléaires, Saclay, F-91191 Gif-sur-Yvette Cedex, France

** Technische Universität, Thermodynamik A, Postfach 202420, D-8000 München 2, Fed Rep of Germany

*** Central Electricity Research Laboratory, Kelvin Avenue, Leatherhead, Surrey KT 22 7SE, U.K.

to the critical point, but it is in precisely this region that critical anomalies in various properties (e.g. heat capacities and thermal conductivities) are best tested against theoretical predictions. Only in the present decade has it become possible to suppress the ordering influence of the earth's gravitational field by conducting the investigations in a microgravity environment. Microgravity, however, is not only useful in suppressing stratification in fluids. It also has value in suppressing convection when such phenomena as critical enhancement of heat transfer or the actual processes of phase separation are being studied.

The liquid-vapour critical point is only one of a number of critical points associated with so-called second order transitions (transitions where a specific property, in this case the density, changes continuously through the transition) [5]. Other examples are the liquid-liquid critical points in binary mixtures [6], the critical points of structural transformation in alloys, the Curie points in magnetic materials and the λ-point for the superfluid transformation in liquid helium.

The behaviour of all these transitions near critical points is formally very similar and to a large extent independent of the nature of the molecular interactions. For example, a number of the parameters which govern the magnitude of critical anomalies are universal. Such universality, besides being scientifically important, has the important practical implication that theoretical predictions confirmed experimentally in one type of system should be applicable to systems which might be difficult or impossible to study directly [7]. Of particular relevance in the present context is the fact that several important effects, which occur in phase transitions in alloys, are much more readily studied in fluid analogues than in the alloy itself.

The phenomena referred to so far are all strictly "near-critical" phenomena and the relevant laws apply and must be tested very close to the critical point. In terms of temperature, this can mean a region within a few tens of mK of the critical temperature. In electrolyte solutions, sedimentation phenomena have been observed much further from the critical point [8].

Although this phenomenon in electrolyte solution is not strictly a near-critical phenomenon, it is closely related to that of stratification in a pure fluid since it is now believed to be a direct consequence of the large compressibility of the solvent [9]. In this case, however, the electrostriction (solvent collapse in the field of the ions) greatly reinforces the extent of stratification, probably by producing both a density and a concentration gradient which act cooperatively. Theories of electrolyte solutions in compressible fluids are very much less advanced than for the true near-critical phenomena – in fact they are only in the very early stages of development. For this reason attention will be focused mostly on the true near-critical phenomena.

It is clear from the foregoing that the current interest in microgravity studies of critical phenomena is primarily scientific. This does not, however, mean there is no technological relevance. Because of the universality of many critical phenomena, advancement in our understanding of one system is likely to advance understanding in apparently quite different fields. It is, therefore, difficult to predict in which areas of technology benefits are most likely to result. Technologies which may benefit are oil recovery, the chemical industry,

lubrication, the preparation of special alloys and the electric power industry. Electrolyte solution studies should help to throw light on a number of currently important problems in the nuclear power industry.

The following provides a short introduction to the problems of critical phenomena, especially with respect to low gravity. The general field has been extensively reviewed by many authors [10–24] in the last decade and the reader is referred to the cited works for a fuller account of both theory and experiment.

B. Fundamentals

B.1. Thermodynamics of Phase Transitions

In most cases a critical point is the terminal point of a line representing transitions which are discontinuous or "1st order" transitions. This end point exhibits many singularities arising from the continuous character of the transition, which is classified as of "2nd order". An example is the gas-liquid critical point in fluids. As demonstrated in the well-known phase diagram (Fig. 1), the vapour pressure curve is terminated by the critical point. At temperatures above the critical only one phase exists; below, at pressures defined by the vapour pressure line, two phases exist, the gas and the liquid phase. Similar behaviour is observed in binary liquid mixtures and in the ferromagnetic-paramagnetic transition for iron at the Curie temperature. The para-phase at a higher temperature is characterized by no magnetization, whereas the ferro-phase at a lower temperature exhibits a spontaneous magnetization.

For a general description of phase transitions the concept of the order parameter, due to Landau, is a useful tool. In pure liquids the order parameter ϕ corresponds to the dimensionless density difference $\phi = (\varrho - \varrho_c)/\varrho_c$ with ϱ_c the critical density; in a liquid-liquid transition, it corresponds to the difference in concentration $\phi = c_A - c_C$ where c_A is the concentration of substance A and

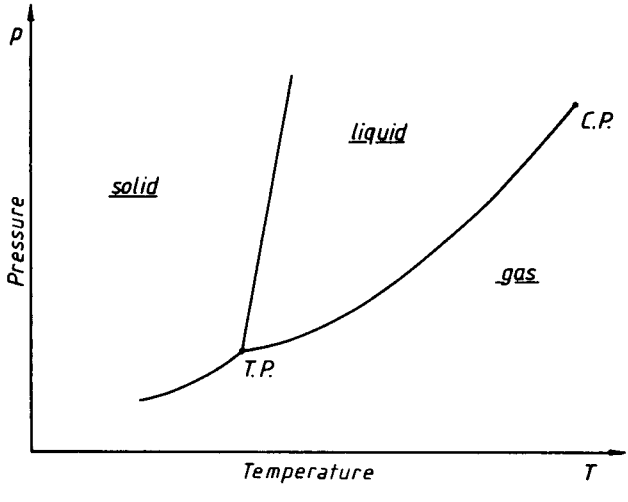

Fig. 1 : Phase diagram of a pure substance. *C.P.* = critical point; *T.P.* = triple point

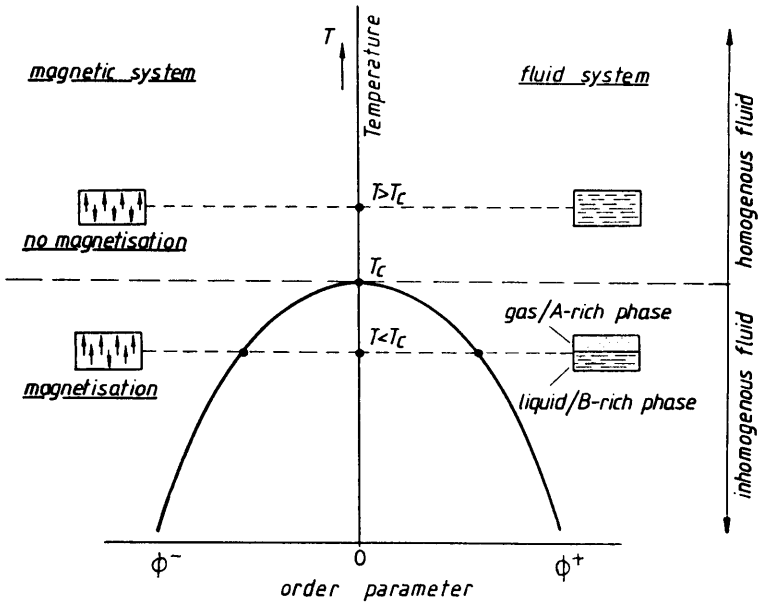

Fig. 2 : Sketch of phase transition in a T, ϕ plot

c_C the concentration of substance A at the dissolution point. In a ferromagnetic system $\phi = M$, which is the magnetization. In a first order transition the order parameter is discontinuous at the transition. For example, the vaporization or condensation of fluids occurs with a spontaneous change of density, or in magnetic systems the spontaneous magnetization occurs at temperatures below the critical.

In a second order transition the order parameter is continuous at the transition point while its derivatives diverge. In Fig. 2 a general sketch of phase transition is demonstrated.

It should be noticed that in a liquid-vapour transition the second order transition occurs only in an experimental cell which is filled at the critical density. Similarly a liquid-liquid mixture must be at the critical concentration. Above the critical temperature the system is homogeneous; below the critical temperature, the system is separated into a gas and liquid phase with different densities. For a liquid-liquid binary mixture of the components $A+B$, the system is decomposed into a A-rich and a B-rich phase.

B.2. Classical Description; Mean Field Theory

The first theoretical description of the gas-liquid phase transition was possible with the van der Waals equation in 1873 [1]. Here the consequences of the attractive and repulsive molecular forces of a real gas are incorporated using two constants. In general, this equation describes the phase transition reasonably well enough for most qualitative purposes.

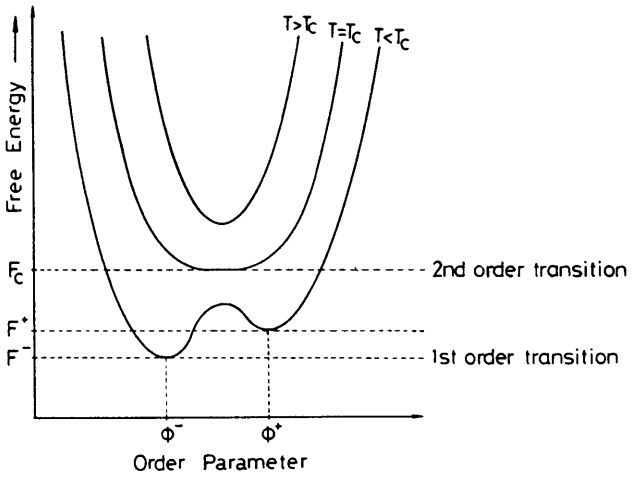

Fig. 3: The Helmholz free energy versus the order parameter ϕ of a pure fluid

With the introduction of the order parameter a more general phase transition was given later by Landau in 1937 [5]. The Helmholz free energy F near the transition is developed as a power expansion of ϕ and T, in which for symmetry reasons only the even powers in ϕ are considered (see Fig. 3).

$$F(T,\phi) = F_0(T,0) + \frac{a}{2}(T - T_c)\phi^2 + \frac{b}{4}\phi^4 + \ldots \,. \tag{1a}$$

If the phase transition of any system can be expressed by eq. (1a), the behaviour of any property which is derived from the free energy is universal. Systems which initially appear to be very different such as the gas-liquid critical point, the liquid-liquid dissolution point of binary mixtures, the Curie point, etc., exhibit the same universal behaviour. The van der Waals equation and the Landau expansion provide an analytical description of the critical point; this behaviour is called "classical".

The equilibrium state of the system is obtained by minimizing F

$$\frac{\partial F}{\partial \phi} = 0 \; ; \qquad \phi[a(T - T_c) + b\phi^2 + \ldots] = 0 \tag{1b}$$

at $T > T_c$ there is only one solution at $\phi = 0$, but two solutions at $T < T_c$,

$$\phi^{\pm} = \pm\left(\frac{a}{b}\right)^{1/2}(T_c - T)^{1/2} \tag{2}$$

The two solutions of eq. (2) describe the coexistence curve of a gas-liquid system, the miscibility curve in a liquid-liquid binary mixture or the magnetization in the ferromagnetic system. From the first derivative of the free energy with respect to the order parameter, field quantities are obtained. These are, in a magnetic system, the magnetic field, in a gas-liquid transition the pressure or equivalently the chemical potential, and in a liquid-liquid mixture the chemical

potential difference between the components A and B. The first derivatives of the free energies exhibit no abnormal behaviour in the properties. For example, the pressure in a gas-liquid system is the same in both phases attaining the critical value, P_c, when the critical temperature is reached.

More abnormal behaviour is shown in the second derivatives of the free energy, here discussed for the example of a gas-liquid transition. These derivatives are very strongly influenced by critical behaviour and, as is later demonstrated, the relevant experimental results obtained on earth are influenced by gravity. The following three-dimensional figures (4 and 5) are obtained from a real equation of state of water which is used for practical calculation purposes [25].

The isothermal compressibility is obtained from the second derivative of the free energy with respect to specific volume

$$\chi_T = \frac{1}{v}\left(\frac{\partial^2 F}{\partial v^2}\right)_T = -\frac{1}{v}\left(\frac{\partial v}{\partial p}\right)_T \tag{3}$$

In any analytical equation which follows a Landau-like expansion at the phase transition, the isothermal compressibility diverges as

$$\chi_T = \chi_0 \tau^{-1} \quad \text{with} \quad \tau = (T - T_c)/T_c \tag{4}$$

In the three-dimensional plot of Fig. 4 the sharp increase of χ_T at the critical point of water is demonstrated.

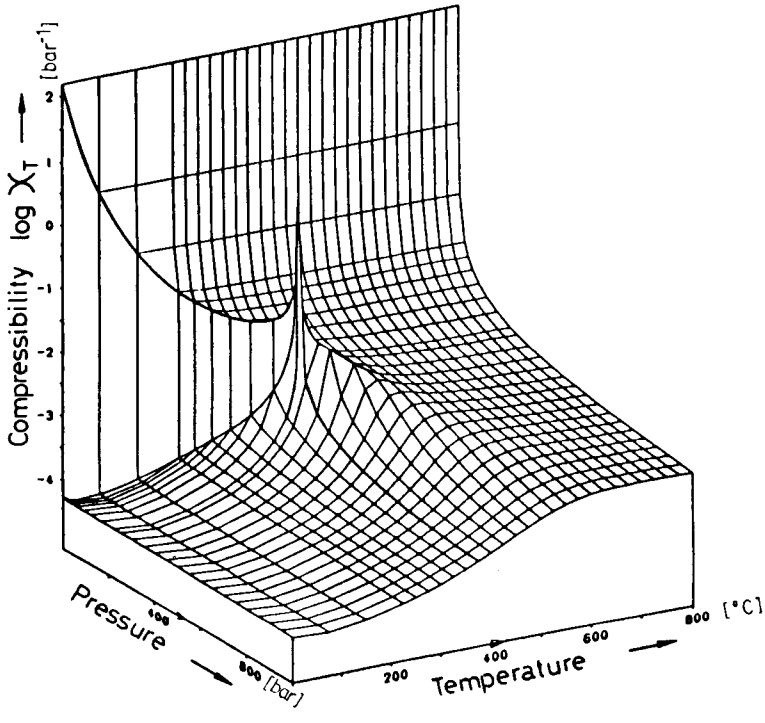

Fig. 4: Isothermal compressibility χ_T over the p, T plane for water

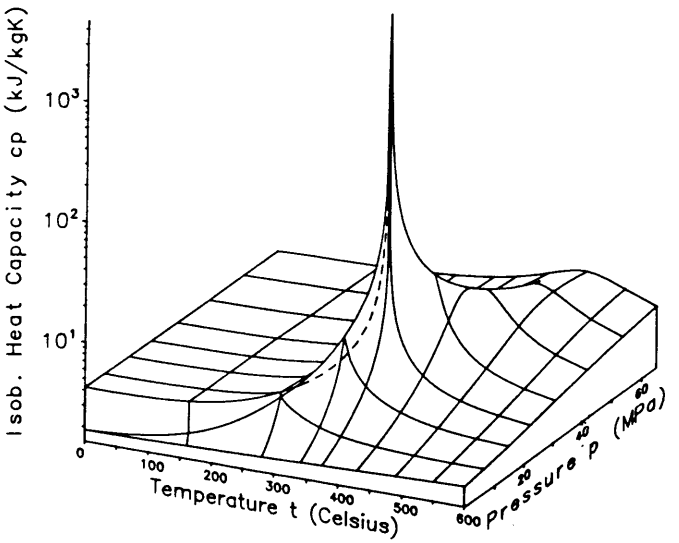

Fig. 5: Isobaric heat capacity c_p over the p, T plane for water

One second derivative of the free energy with respect to temperature is the heat capacity at constant pressure. As seen in Fig. 5, this also diverges strongly at the critical point. According to the classical description, the heat capacity at constant volume is expected to be abnormally high but not divergent.

B.3. Scaling Laws

At the turn of the century, several experimental results, especially those involving the coexistence curve of fluids, were found to exhibit a discrepancy in the classical description. For instance, the coexistence curve is better described by experiments with a power of the order of $1/3$ instead of $1/2$ as implied by eq. (2). This observation has been confirmed during the past 20 years by more exact experiments of different thermophysical quantities. From these it follows that classical exponents are not correct at the critical point. Therefore, in the past few years, strong theoretical and experimental efforts have been made to determine the power laws of the respective quantities on thermodynamic trajectories like isochores and isotherms. Their exponents are called the critical exponents and they describe the critical behaviour very close to T_c.

The following power laws and exponents are used for the order parameter at $T<T_c$

$$\phi = \phi_0 \tau^{\beta} \tag{5}$$

For the gas-liquid transition in pure fluids this is equal to the density difference on the coexistence curve

$$\frac{\varrho_l - \varrho_g}{\varrho_c} = B_0 \tau^{\beta} \tag{6}$$

and for binary liquid mixtures the difference in the concentration of substance A in the phase 1 and 2 below the dissolution point is given by

$$c_{A_1} - c_{A_2} = B_c \tau^{\beta} \tag{7}$$

On the critical isotherm, in gas-liquid transitions, the difference in the chemical potential is given by the power law

$$\frac{\mu - \mu_c}{\mu_c} = D_0 \phi |\phi|^{\delta - 1} \tag{8}$$

The isothermal compressibility or susceptibility is given by

$$\chi_T = \Gamma \tau^{-\gamma} \tag{9}$$

The isochoric specific heat capacity represents the power law

$$C_v = A_0 \tau^{-\alpha} \tag{10}$$

If there exists an interface between two coexisting phases with a surface area A, the first derivative of the free energy with respect to the surface area defines the interfacial or surface tension. This quantity exhibits a universal behaviour with a power law when approaching the critical temperature

$$\sigma = \sigma_0 \tau^{\mu} \tag{11}$$

The values of these critical exponents which follow from the classical analytical description, and the experimental values, are compared in Table I with the results of the Renormalization Group (R.G.) theory. This will be discussed in the following section. It may be seen that there are large discrepancies between the classical values and the experimental ones. The values of the R.G. theory are now widely agreed on, although some problems remain. This is especially the case at the liquid-vapour critical point for pure liquids, where the experiments are influenced by stratification and convection effects, as will be discussed later.

Table I: Comparison of values of critical exponents

Critical Exponents	β	δ	γ	α	ν	μ
Experiments (pure liquids)	0.32–0.36	4.2–4.6	1.15–1.26	0.110–0.098	0.625–0.635	1.26–1.3
Classical theory	1/2	3	1	0	1/2	1.5
Renorm. Group theory	0.325	4.815	1.240	0.110	0.63	1.26

These critical exponents are not independent of each other; they are interrelated by the so-called Scaling Laws, which can be derived from thermodynamic relations and have been confirmed by theory and experiment. The most important Scaling Law relations are

$$2\beta + \gamma = 2 - \alpha$$
$$\beta(1 + \delta) = 2 - \alpha$$
$$3\nu = 2 - \alpha$$
$$2\nu = \mu \tag{12}$$

The exponent ν is that of the correlation length and is defined by eq. (13) in the next section. It should be noted that only two exponents are independent and all exponents are related to ν. Further it is worth noticing that, as for the exponents, there exist universal relations between amplitudes, so that only two of them are independent.

B.4. Fluctuations and Correlations

During the first optical observation of the critical point by Andrews (1869) [2] with a relatively primitive apparatus, the temperature control in the experiment was sufficiently fine to allow critical opalescence, the enhanced scattering of light by the fluid, to be observed for the first time. This opalescence was evidence to Andrews of large scale density fluctuations in the fluid; they are linked to the large compressibility in the critical region and Andrews described the critical point as a point of instability.

Andrews's concept, that the essence of critical behaviour is found in the nature of the fluctuations and in the increasing instability of the system approaching the critical point, is the basis of modern day understanding of critical phenomena. It is actually known to be a universal behaviour of phase transitions of second order.

In approaching the critical point, large scale density fluctuations or, more generally, fluctuations of the order parameter, develop throughout the fluid. These fluctuations are correlated, the spatial extent of the correlations being characterized by the correlation length ξ. Thus the specific nature of the critical region involves the appearance of a new characteristic distance, which is much larger than the average distance between particles (see Fig. 6).

Approaching the critical point by lowering the temperature from above T_c, the correlation length diverges as

$$\xi = \xi_0 \tau^{-\nu} \tag{13}$$

Once the correlation length ξ has become much larger than the range of intermolecular forces, the specific microscopic features of interaction become irrelevant to the description of the critical behaviour: all that matters is the structure of the correlations, namely, the dimensionality of the physical space d and the tensor characters, n, of the correlated fluctuating quantity, the order parameter. The principle of universality states that the only relevant attributes of the system are d and n, and that diverse physical systems can be grouped into universality classes, according to their values of d and n. All systems belonging to the same universality class display the same thermodynamic behaviour. It should be noted that, for liquid-vapour equilibria in the earth gravitational

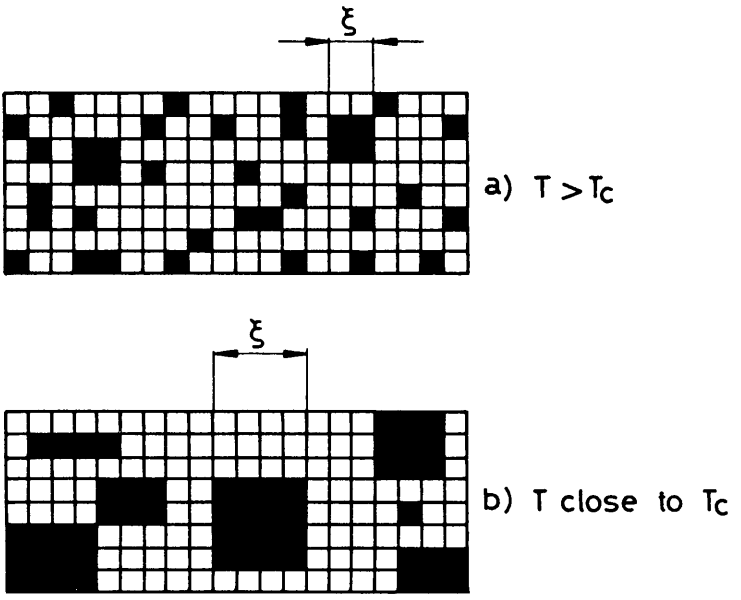

Fig. 6: Increase of the correlation length ξ when approaching T_c, in a 2-dimensional model **a)** $T \gg T_c$, **b)** $T \geq T_c$

field, it is necessary to consider correlations which differ with respect to the gravity direction [26, 27].

As mentioned previously, for the gas-liquid system, the order parameter ϕ is the density difference $(\varrho - \varrho_c)/\varrho_c$, a scalar with $n = 1$. The order parameters applicable to the binary liquid-liquid dissolution point of a mixture and the Curie point of a ferromagnet are also scalars. The dimensionality of these systems is $d = 3$, so that all belong to the 3–1 universality class. The theoretical model corresponding to this class is the three-dimensional Ising model. (A two dimensional illustration of increasing correlation length near T_c is provided in Fig. 6). For the superfluid transition of He, n is a tensor of character 2, so that this system belongs to the 3–2 class.

B.5. Renormalization Group Approach

The fact that classical, or mean field theories do not fit the experimental results near the critical point has been known for a long time. The basic reason is that the mean field approach is of macroscopic order. This means that the discrete molecular structure is neglected and any infinitesimal element of volume is always supposed to be large enough to contain a large number of particles. The fluctuations of the order parameter $\phi(\boldsymbol{r})$, with $\boldsymbol{r}$ a positional variable, is a quantity attached to a small – but a macroscopic – volume of size L^d, with $d = 3$, located at the position $\boldsymbol{r}$, which is supposed to be at thermal equilibrium. Such an order parameter requires that the correlation length ξ is smaller than the size L. This is not possible close to T_c, where ξ diverges. The underlying

idea of the Renormalization Group approach to critical phenomena is to take not only the average values of $\phi(r)$, but also fluctuations over all scales L up to $L \sim \xi$ into account.

The Renormalization Group approach (Wilson and Kojut in 1974) [15, 28] consists of breaking down an intractable problem with multiple scales of length into a sequence of smaller problems, each of which is confined to a simple scale of length. One version of the method, called the block-spin transformation, is described here for illustration applied to a ferromagnetic spin system. First the lattice is divided into blocks of a few spins each. Then each block is replaced by a single spin whose value is the average of all spins in the block. In this way a new lattice is created with, for example, three times the original lattice spacing and one-third the density of spins. Finally the original scale is recovered by reducing the dimensions by a factor of 3. The procedure must be carried out for all configurations of spins in the original lattice, so that a probability can be found for every configuration of the block spin. This modern concept is able to explain the experimental finding that the power laws, which describe the various thermodynamic quantities near the critical point, are governed by the same exponents.

The behaviour near T_c will not be dependent on the particular nature of the molecular interactions, but on the fluctuations of the order parameter, which is universal in all systems. From these it follows that the large increase of the correlation length of these fluctuations is universal too, only the amplitude ξ_0 of eq. (13) is an individual constant. Hence, for example, the calculations performed on the ferro-paramagnetic transition, with an Hamiltonian describing its free energy, could be applied to a gas-liquid or fluid mixture as well.

B.6. Transport Properties

In a liquid-vapour system [29] the thermal conductivity λ and the shear viscosity η exhibit an enhancement in the vicinity of the critical point. In binary mixtures the thermal conductivity is not divergent but the mass conductivity, or the diffusion coefficient, exhibits a critical reduction. The overall behaviour of transport properties generally shows a rather weak enhancement. In order to describe this critical behaviour, the transport properties are separated into a normal, or background, term and a critical term of the enhancement. For instance the thermal conductivity is written as

$$\lambda = \bar{\lambda} \pm \Delta\lambda \tag{14}$$

Outside the critical region, the thermal conductivity is identified alone with the normal thermal conductivity $\bar{\lambda}$; inside the critical region by adding the enhancement $\Delta\lambda$. The viscosity η has been handled in a similar fashion. The dynamic Mode Coupling and Renormalization Group theories predict that the critical enhancement is a function of the correlation length and therefore of the thermodynamic variables. Furthermore, it is expected to show scaling behaviour. Thus the enhancement of the thermal conductivity diverges asymptotically at the critical point as

$$\Delta\lambda = \frac{\Lambda}{6\pi\eta\xi}\frac{k_B T^2}{\varrho^2}\left(\frac{\partial p}{\partial T}\right)^2_{\varrho}\chi_T \tag{15}$$

For the viscosity

$$\Delta\eta \sim \xi^{\chi} \tag{16}$$

Here k_B is the Boltzmann constant, Λ is a universal constant and χ a universal exponent independent of the nature of the fluid, calculated as $\chi \approx 0.054$. The exponent χ has also been calculated from a perturbation expansion, yielding 0.065. The viscosity has only a very weak singularity and to date the critical exponent is not universally accepted.

From eq. (15) the temperature dependence of the thermal conductivity enhancement can be derived as

$$\Delta\lambda \sim \eta^{-1}\xi^{-1}\chi_T \sim \tau^{\nu(\chi+1)-\gamma} \tag{17}$$

The enhancement of the thermal conductivity with $\tau^{-0.58}$ is found experimentally.

The mass diffusion coefficient for binary mixtures can be derived from the Einstein relation with the correlation length as a typical scale for near-critical behaviour [30].

$$D = \frac{k_B T}{6\pi\eta\xi} \tag{18}$$

Thus the diffusion coefficient converges as

$$D \sim \tau^{\nu(\chi+1)} \tag{19}$$

This result is confirmed by more accurate theories and experiments [6].

The thermal diffusivity ratio is defined as

$$D_{th} = \frac{\lambda}{\varrho C_p} \tag{20}$$

Considering the well-known relationship [5]

$$C_p - C_v = TV\chi_T\left(\frac{\partial p}{\partial V}\right)^2_V \tag{21a}$$

one realizes that C_p diverges as χ_T, i.e. with exponent $\gamma \simeq 1.24$. The critical part (eq. (20)) will, therefore, behave as

$$\Delta D_{th} \sim \tau^{\nu(\chi+1)} \tag{21b}$$

and it will go to zero when approaching T_c. Long times to reach density equilibrium are thus observed close to the critical point.

B.7. Approach to Equilibrium

In every individual experiment the approach to a critical state is a transient process governed by the conservation laws. The anomalous behaviour of the transport properties involves non-linear partial differential equations in which the temperature variation of the properties has to be taken into consideration. Differential equations of this kind can only be solved numerically with the given initial boundary conditions of the experimental process. Therefore, only some simple approaches to this complicated problem follow.

The smallest scale in a sample near its critical point is the correlation length ξ. The dimensionless time for transient processes is the Fourier-number. If we assume the fluctuations to be a sphere with a diameter ξ, the respective Fourier-number is $\mathrm{Fo} = tD/(\xi/2)^2$, with t the actual time and D a diffusion constant (D_{th} for the heat transfer).

For this simple model the corresponding energy equation can be analytically solved and the time for temperature equilibration within a fluctuation calculated. To simplify matters we write $\mathrm{Fo} = 1$, which means that a sudden temperature change on the wall of the sphere is adjusted in the centre within 10^{-4} of the initial change of the dimensional temperature; the time required to attain equilibrium can then be estimated as

$$t = \frac{(\xi/2)^2}{D_{th}} \tag{22}$$

It is generally assumed that this is, in the same way, the intrinsic lifetime of a fluctuation. We use as an example, the liquid-vapour system SF_6, and measured values of the thermal diffusivity for the critical isochore [31]. One achieves the equilibration time of a fluctuation in a time t_ξ

$$t_\xi \approx 4.4 \times 10^{-14} \cdot \tau^{-2} \quad \text{sec} \tag{23}$$

and for $\tau = 10^{-6}$ (0.3 mK from T_c), the equilibrium time is $t = 0.3$ s. For a bulk sample cell the solution of the energy equation is more complicated. In the differential equation the change of the properties with temperature and density in a differential element has to be considered including all the experimental conditions. In the gravity field the local change of density by the stratification process must be allowed for using an equation of state. In experiments it has been observed that thermal equilibrium is adjusted relatively fast but the density stratification due to a diffusion process takes many hours. Under microgravity conditions, special care should be taken to ensure equilibrium. In particular a critical sample can be stirred. This process is however of limited value in the sense that the velocity gradient s at the scale of the order parameter fluctuations should be negligible. Hence the condition $s \cdot t_\xi \ll 1$ must be fulfilled [32] with t_ξ as the intrinsic lifetimes of the fluctuation as given by eq. (23).

B.8. Phase Separation Process, Nucleation and Spinodal Decomposition

The region of stability of a fluid or a mixture of fluids is determined by the location of the minimum free energy in the plane T, ϕ, (Fig. 7): $\partial F/\partial\phi = 0$, which determines the coexistence curve. The region inside this curve is unstable and can be divided, according to the classical mean-field theory, into a region of metastability, where the 2nd derivative $\partial^2 F/\partial\phi^2 > 0$, and a region of instability, where $\partial^2 F/\partial\phi^2 < 0$. The limit between these regions is known as the spinodal line: it is where $\partial^2 F/\partial\phi^2 = 0$ [33].

When a system, initially in the one-phase region, is quenched into the unstable region, its phase separates. One classically distinguishes two regions according to whether it is quenched in the metastable or in the unstable region:

a) In the metastable region, phase separation is initiated by a nucleation process, through spontaneous fluctuations (homogeneous nucleation) or impurities (heterogeneous nucleation). When an embryo increases in size, the free energy can be changed for two reasons. The first is the decrease in the bulk energy i.e. the amount $\frac{4}{3}\pi r^3 \Delta F_v$, where ΔF_v is the free energy change per unit volume related to the phase separation, r being the embryo radius. The second is the cost in energy to form an interface, i.e. $4\pi r^2\sigma$, where σ is the interfacial tension between both phases. As can be seen in Fig. 7, ΔF_v is always negative, whereas σ is always positive; thus, the resulting energy variation

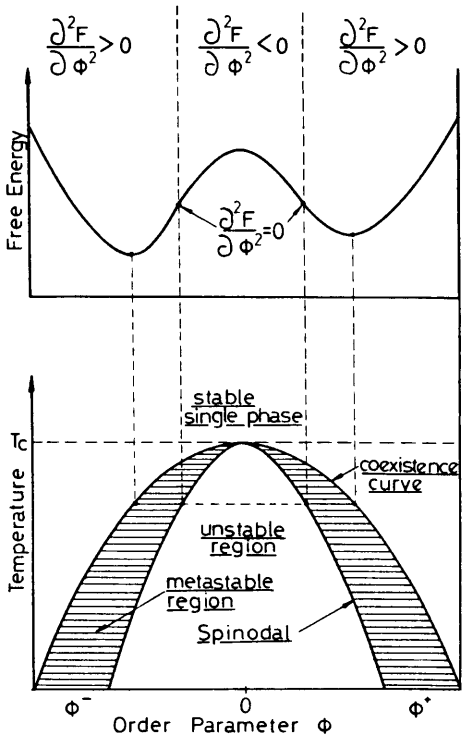

Fig. 7: Schematics of phase equilibria

$$\Delta F = 4\pi r^2 \left(\sigma - \frac{r}{3|\Delta F_v|} \right) \tag{24}$$

is a function of the size of the embryo, and exhibits a maximum for the critical radius r^*, a radius above which the embryo can only be stable and grow

$$r^* \sim \frac{3\sigma}{|\Delta F_v|} \tag{25}$$

The growth law of the embryo is dependent on its size and on the number of droplets in the solution; usually it follows a Lifshitz-Slyozov growth [34], where $r \sim t^{1/3}$.

b)In the unstable region, no nucleation barrier exists to prevent the growth of the fluctuations, and the system is unstable. Although most of these fluctuations can grow, they do not exhibit the same growth rate; the fastest ones are precisely those whose size is of the order of the correlation length ξ pertaining to the fluctuations of the system at that temperature. Thus a typical wavelength $\lambda m \sim \xi$ is rapidly imposed on the system, giving rise to a well-defined ring when scattering techniques (light, X-rays or neutrons) are used.

Depending on the volume fractions (v) of the droplets, a growth by diffusion and coalescence can be observed when v is small: $\lambda m \sim t^{1/3}$. Alternatively, if the phase separation occurs near the critical point, where the volume fraction is nearly 50 %, interconnected (percolated) structures appear. This accelerates the phase separation process through capillary hydrodynamic instabilities, making valid the growth law [35]:

$$\lambda m \sim t \tag{26}$$

It is obvious that, under one-g conditions, only the early stages of such nucleation and spinodal decomposition growth laws can be observed; convection and sedimentation processes severely affect the growth, transporting the denser phase to the bottom of the samples. Concerning hydrodynamics, the question arises therefore as to the relative influence of capillary flows and gravity-driven flows.

B.9. Adsorption and Wetting

(See also in this book the contribution of G.H. Findenegg and M.M. Telo da Gama, Chapter VI, "Wetting and adsorption phenomena").

All the properties discussed above were bulk properties and systems were assumed to be of infinite spatial extent. We will now consider the influence of the walls of the container. The wall can be regarded as an extra phase, so the 1-phase region becomes a 2-phase region, and the 2-phase region a 3-phase region. A wall (W) modifies the potentials at the surface and is in some ways analogous to a field for magnetic systems.

Let us consider (Fig. 8) a system with 2 components or phases A and B and a wall W. For pure fluids A will be the liquid, and B the vapour.For mixtures,

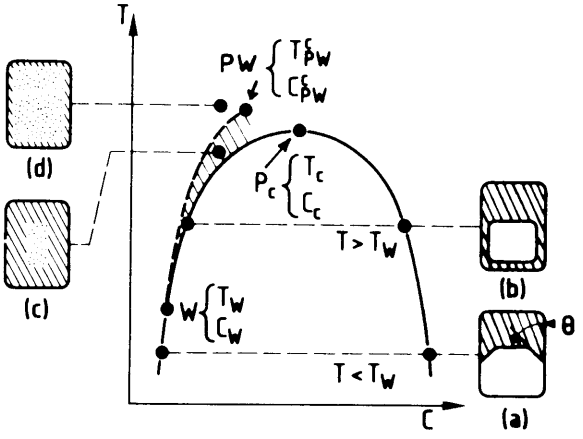

Fig. 8: Different wetting or adsorption regimes for pure or binary fluids. P_c: critical point; PW: critical prewetting point; W: wetting transition point; $W - PW$: prewetting line. In (a) (b) (c) (d) are the different cell configurations

A and B will be the components, and W could be the vapour as well as the wall of the container.

We assume A to be the component the more attracted by W. Near W there is a competition between the attraction of the wall and the corresponding variation of the bulk intermolecular potential. Several possibilities of weak or strong adsorption will result, according to the balance of energy, i.e. according to the location of the system in its phase diagram (T, ϱ) or (T, c) [36].

B.9.1. In the Two-phase Region: Wetting

Let the system be on the coexistence curve, where two phases of different composition coexist. Within ordinary gravity conditions a meniscus separates the A-rich (A) and B-rich (B) phases. The meniscus is bent near W with an angle determined by the Antonov rule

$$\sigma_{A^+B^+} \cos\theta = \sigma_{A^+W} - \sigma_{B^+W} \tag{27}$$

$\sigma_{A^+B^+}$ is the interfacial tension between the A^+ and B^+ phases. It obeys a power law, (eq. (11)).

σ_{A^+W}, σ_{B^+W} are proportional to the density of the A^+ and B^+ phases, respectively, i.e. for the difference we obtain

$$\sigma_{A^+W} - \sigma_{B^+W} \sim \tau^{\beta} \tag{28}$$

Therefore $\cos\theta$ varies with τ as:

$$\cos\theta \sim \tau^{\beta-\mu} \sim \tau^{-1} \tag{29}$$

i.e. diverges at T_c! A temperature T_W therefore exists where $\cos\theta = 1$ holds. From T_W to T_c, the A^+ phase wets the wall completely. The transition from

partial wetting ($T<T_W$) to complete wetting ($T_c>T>T_W$) is called the wetting transition, which, experimentally, has so far only been found to be of 1st order [37].

In the complete wetting regime, the width of the A^+ layer, located between the B^+ phase and the wall, depends on the relative importance of gravity and the interaction forces $A-W$. In particular, the van der Waals forces lead to a film thickness (L) versus height (h), which should vary as $L\sim h^{1/3}$, whereas one expects a logarithmic dependence when neglecting the van der Waals interactions $L\sim \log h$ [37].

Note that this wetting behaviour can be somewhat complicated by the influence of long-range forces such as the van der Waals forces. This might lead to some "dewetting" phenomena near the critical point [38].

B.9.2. In the One-phase Region: Prewetting

The wetting transition is continued into the single-phase region by a prewetting line (Fig. 8), which separates a region of A-weak adsorption on W ("thin") from a region of A-strong adsorption ("thick"). The corresponding transition is expected to be generally 1st order. The transition line should start tangentially at the coexistence curve at the wetting transition and finish at a 2nd order transition end point PW.

B.9.3. Near the Critical Point : Critical Adsorption

Because of the susceptibility divergence near the critical point, any pertubation of the chemical potential will induce an order parameter perturbation on a length scale comparable to the correlation length ξ. This leads to an anomalous adsorption. The concentration profile of constituant A is universal, with Z the distance to the wall, the excess concentration is expected [39] to vary as $Z^{-\beta/\nu}\sim\sqrt{Z}$ at T_c.

B.10. The λ-Point of Helium

The λ-point of He ($T_\lambda\approx 2.17$K) is a good example of a very sharp 2nd order phase transition. Indeed, superfluid ^{4}He is a quantum fluid and the order parameter is a wavefunction characterized by an amplitude and a phase. This transition with $d=3$, $n=2$ does not belong to the same universality class as the usual critical point in fluids ($d=3$, $n=1$). As a consequence, the values of the critical exponents are different. The λ-point offers interesting experimental possibilities:

- The system is superfluid below the transition, making the thermal relaxation times short.
- The isothermal compressibility diverges weakly; however gravity reduces the range of study through the influence of hydrostatic pressure.

On earth accurate data can be obtained down to reduced temperatures of $\tau=(T-T_\lambda)/T_\lambda\sim 10^{-6}$. This limiting value is mainly due to the hydrostatic

pressure influence. Experiments in a 10^{-4} g environment would allow a reduced temperature of 10^{-8} to be obtained – i.e. the critical point could be approached very closely [40].

B.11. Electrolyte Solutions

Electrolyte solutions exhibit unusual behaviour in a region very much further from their liquid-vapour critical points. Phenomena quite different from those discussed so far are involved. The abnormal behaviour of such solutions is dominated by the phenomenon of electrostriction; this is the local compression of the solvent in a strong electric field such as that near an ion. If the solvent's compressibility is high, its density near an ion can be significantly increased. Very unusual thermodynamic and transport properties of the ions result [41–43].

In 1960, Corwin, Bayless and Owen [8] reported that at temperatures well above the critical, aqueous solutions of sodium chloride had appreciably higher conductances at the bottom than at the top of the conductance cell. No explanation was offered and their finding appears to have been largely disbelieved or ignored. It now seems likely [9] that their finding is a direct consequence of the local increase in density near an ion leading to significant sedimentation. The relationship between the concentration and the conductance gradient is not likely to be straightforward in a strongly sedimented solution, since all the forces influencing the conductance are likely to vary with vertical position.

The established theories of electrolyte solutions (the Debye-Huckel theory of activity coefficients, the Onsager conductance law and the Bjerrum theory of ion association, as well as their subsequent improvements) are all based on the assumption that the solvent is incompressible. In aqueous solutions, marked deviations from this requirement are apparent 75°C below as well as above the critical point of water (374°C). The theories need to be modified at a quite basic level if they are to be used to obtain useable equilibrium constants and related thermodynamic data from experimental results on compressible solutions.

The principal motivation for studying electrolyte solutions near the critical point under conditions of microgravity is the provision of data which can be used to check such improved theories. Clearly it is necessary to undertake at least some of the experiments under conditions where stratification can be ignored. Conductance is one of the most useful techniques available and is the only one which has been extensively employed in studying aqueous electrolytes under near critical conditions.

Conductance studies have also been made on binary liquid mixtures of which one component is polar [44]. These systems exhibit a large decrease of conductance near the liquid-liquid critical point. This phenomenon is observed very close to the critical temperature and seems to be a "true" critical phenomenon arising from the interaction of charge carriers with concentration fluctuations.

C. Why Microgravity ?

C.1. Influence of Compressibility

The isothermal compressibility χ_T in a liquid-vapour transition diverges at T_c according to eq. (9). Therefore, under ordinary gravity conditions the fluid is compressed under its own weight and no longer remains at the critical density in the bulk. Density stratification is the result of this high compressibility and within a sample cell of critical bulk density, density gradients are exhibited which are governed by

$$\left(\frac{\partial \varrho}{\partial z}\right)_T = -\varrho g \left(\frac{\partial \varrho}{\partial p}\right)_T = \varrho^2 g \chi_T \tag{30}$$

with z as the vertical coordinate in the opposite direction to the gravity vector.

From this, it follows that all measurements of critical properties obtained from bulk properties are necessarily average, integrated values and become meaningless close to T_c. Optical measurements, using a refractometer or interferometer, can be used to analyse such density profiles (see Fig. 9) [45].

These methods provide the closest measurements to T_c of the coexistence curve, critical isotherm and compressibility. But even then there is a range of $\pm(1\text{–}2)$ mK of T_c and of 4 % of the critical density which cannot be resolved, because the refractive index gradient $(\delta n/\delta z)$ diverges when the critical density

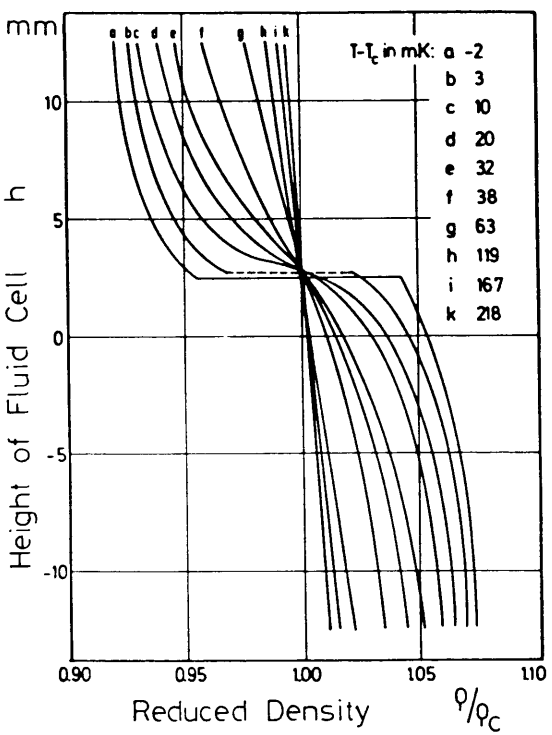

Fig. 9: Density profiles of N_2O measured with a refractometer [42]. (Reprinted with permission from Journal of Physical Chemistry **85**. Copyright (1981) American Chemical Society)

at T_c is approached. In reality, in a sample at T_c, only a layer of the height of the correlation length (approximately 10^{-6}m) is in critical condition, so even in a cell of 1 mm height only about 1 ‰ of the mass is really critical.

Nearly all properties in the liquid-vapour transition are influenced by the compressibility and the gravity effect, so that in theory our knowledge of critical behaviour is all based on an extrapolation to T_c and to ϱ_c. In practice, strongly anomalous properties can be measured sufficiently well on earth but weak anomalies (exponent < 0.5) should benefit from a micro-g environment [7, 46]. These properties include shear viscosity, dielectric constant, refractive index and sound velocity in addition to C_v. The somewhat related problem of stratification in electrolyte solutions has been dealt with in Section B.11.

C.2. Influence of Isochoric Expansion Coefficient

From thermodynamic identities it follows that the isochoric thermal expansion coefficient is directly related to the compressibility; this means that the expansion coefficient diverges in the same way as the compressibility. Convection instabilities are governed by the Rayleigh number

$$\mathrm{Ra} = \frac{1/\varrho(\partial\varrho/\partial T)_p H^3 \Delta T}{\eta D_{th}} \tag{31}$$

Here H is the characteristic linear dimension in the direction of the gravity vector and ΔT a temperature difference between a wall and the bulk fluid, or between two walls. The other properties have all been defined previously. The Ra-number diverges very strongly approaching T_c.

$$\mathrm{Ra} \sim \tau^{-(\gamma+\nu)} \sim \tau^{-1.87} \tag{32}$$

Thus even very small temperature differences induce convection in a near critical sample and disturb the equilibrium conditions. Each change of temperature is accompanied by convection and a long time is necessary for the equilibration process of the density stratification. In space convection is suppressed, nevertheless temperature inhomogeneities be equilibrated fast by conduction, because of the diverging thermal conductivity at T_c.

C.3. The Phase Separation Process

When a fluid system (gas-liquid or liquid-liquid) undergoes a phase separation by nucleation or spinodal decomposition under earth gravity conditions, the process is rapidly influenced by convection. In the final stages of the separation the denser phase sinks to the bottom of the container although wetting forces may partially modify this picture.

Due to the sedimentation process, late spinodal or nucleation stages cannot be reached. This prevents a clear understanding and a test of the mechanisms proposed for the phase separation. In particular the role of interfacial tension remains uncertain.

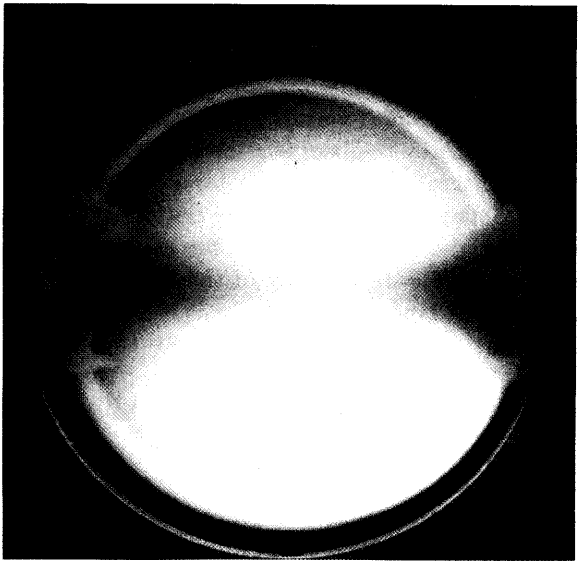

Fig. 10: Phase separation (gas-liquid) in the refrigerant R12 on earth

Figure 10 shows a photograph of a critical sample of the refrigerant R13 slowly cooled from $T > T_c$. In the middle of the picture, the typical critical opalescence is observed, while the fog from both sides in the centre demonstrates the phase separation as a dispersion of droplets and bubbles. In the next stage the phases will be decomposed by sedimentation.

C.4. Wetting Layers

The wetting layer thickness is governed by capillary forces including microscopic (van der Waals) forces, balanced against the action of gravity; it is therefore very g-dependent. A simple way to understand that it will asymptotically vanish as the critical point is approached is to consider the Laplace radius R (Fig. 11)

$$R = 2\left[\frac{\sigma}{g \cdot \Delta\varrho}\right]^{1/2} \tag{33}$$

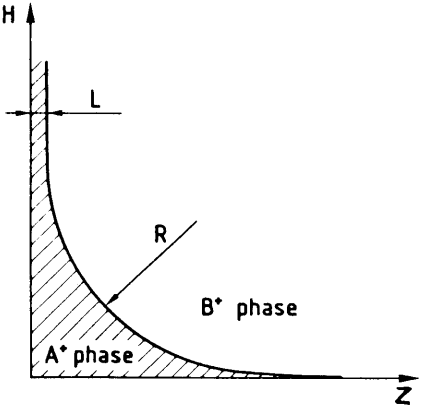

Fig. 11: Film thickness L and Laplace radius R. H is directed vertically and Z is perpendicular to the wall.

Near T_c, σ and $\Delta\varrho$ go to zero according to eqs. (11) and (6). Therefore

$$R = \tau^{\nu-\beta/2} \approx \tau^{1/2} \tag{34}$$

and will always go to zero at T_c; the only way to observe a thicker wetting layer is to reduce or eliminate gravitational accelerations.

Note that when g goes to zero, the layer becomes so large that its thickness is no more governed by residual gravity and/or microscopic forces, but by volume fraction considerations. Then it is the g-dependence of the layer thickness which is of interest rather than the $g \simeq 0$ aspect.

Finally the transition from complete wetting to incomplete wetting should lead to interesting patterns, since the fixed volume fraction of the phases will compete with the fact that the two phases should coexist at the walls of the cell.

C.5. Interface Stability and Capillary Waves

Let us consider a situation as in Fig. 12 where the phase A^+ wets completely the walls of the container in a weak gravity field. The interface A^+B^+ is submitted to capillary wave fluctuations of amplitude ϱ. Such fluctuations are damped by gravity. Although in a microgravity experiment the capillary waves are indeed enhanced, they cannot diverge because of the finite size of the drop containing the phase B^+, which limits their amplitude.

The influence of such fluctuations is not clear at the moment, since the surface tension value can be affected, as well as the process which leads to the formation of an interface [47] during the phase separation.

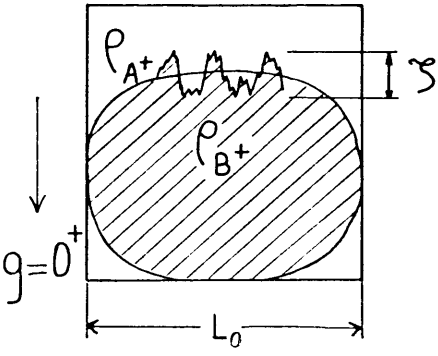

Fig. 12: Capillary waves and fluctuating interface in a low-g environment

In some cases an instability can occur if $\varrho_{A^+} > \varrho_{B^+}$ as shown in Fig. 12 (Rayleigh-Taylor instability) [48]. Simple calculations show that the interface is stable only if the Laplace length is such that $R \geq L_0$, with L_0 the dimension of the container. Then the simple picture of Fig. 12 could break down near T_c in a microgravity environment, where, moreover, the fluctuations in amplitude and direction of the residual g (i.e. g-jitter) might allow instabilities to develop.

D. Status of Experimental Investigations

A number of experiments on critical phenomena have already been performed in microgravity; a few during space shuttle missions in Spacelab D-1 and some in sounding rockets within the German and ESA/TEXUS program. Sounding rockets provide microgravity levels better than 10^{-4} during the ballistic flight of approximately 6 minutes. A number of experimental proposals to various national and international space agencies have been made and are awaiting flight opportunities.

D.1. Specific Heat in a Liquid-Vapour Transition

During the D-1 Mission in autumn 1985 measurements of the internal energy at the liquid-vapour critical point of SF_6 were performed. In a four stage scanning-ratio calorimeter (Fig. 13) mounted in a high- precision thermostat (HPT) the energy necessary to heat up a critical sample of SF_6 from $T - T_c = -100\,\mathrm{mK}$ up to $T - T_c = +100\mathrm{mK}$ was measured. The sample cell is disc-shaped, 30 mm in diameter and 1 mm thick. During the mission, four different temperature ramps between 3.6 to 100 mK/h were employed in order to study the influence of relaxation effects on the apparent specific heat [49,50].

For theoretical modelling of critical phenomena the isochoric specific heat is one of the most important properties. Measurements of this quantity are only possible in the bulk fluid and due to the high compressibility the results are strongly influenced by gravity. To date only extrapolations of this property to zero-gravity behaviour have been possible. The effect of gravity is demonstrated in Fig. 14, which shows measurements of the sample with 1 mm and 15 mm height under one-g conditions. The sample cell can be turned, so that different

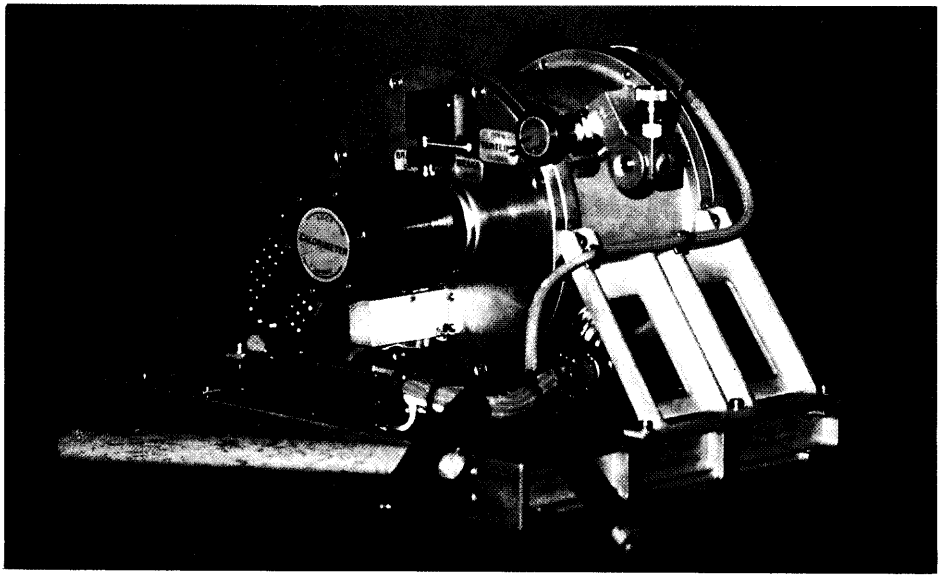

Fig. 13: The calorimeter in the HPT (D-1)

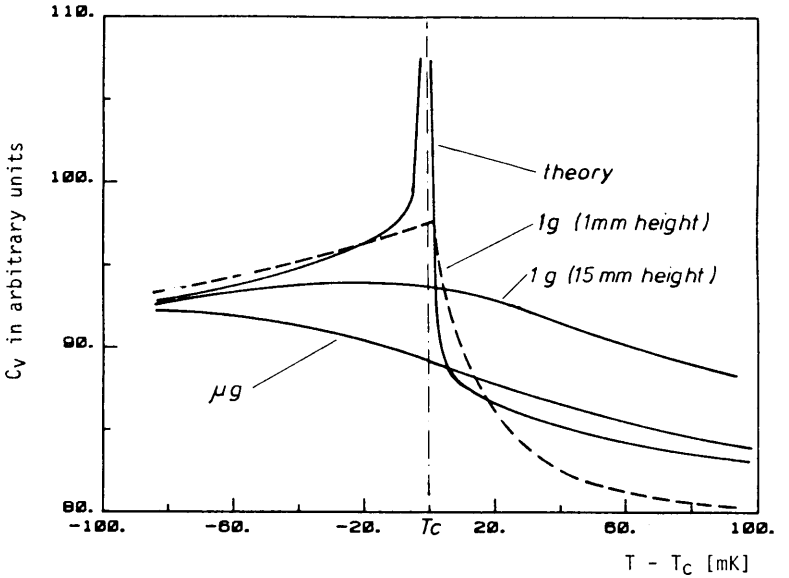

Fig. 14: Specific heat measurements in space compared with one-g measurements at different heights of the cell, 1 mm and 15 mm, and the prediction of theory. The absolute value of C_v is arbitrary

hydrostatic heights are realized using the same cell. Generally it is believed that, as the theory predicts, the peak is more rigorously developed under zero-gravity. The experiment was expected to measure really the specific heat at constant critical density.

However, the measured micrc-g curves are surprisingly low and even smoother than on earth. The peak predicted by the theory was degenerated to a hump [50, 51]. These quite unexpected results cannot be explained by malfunction of hardware: after landing, the experiments were repeated in the original flight configuration and the critical peak was again observed. Wrong filling of the specimen cell or impurities of the substance cannot explain this result [51]. The thermal equilibration seems not to be greatly retarded, as discussed in the following chapter, and therefore the mechanism of the mass transport from the liquid to the gaseous phase during heating and a possibly density inhomogenity could be the only effects for the explanation at the moment. This finding is not well understood and is still under investigation.

D.2. Phase Separation Process

As described earlier, microgravity allows the study of the process of phase separation by spinodal decomposition and nucleation. The sedimentation, which immediately follows the phase transition, can be suppressed under micro-g conditions, and the process is only driven by pure mass diffusion and interface instabilities. The process has been studied after a temperature quench by optical observation of the cell and using a light scattering method after a temperature quench.

D.2.1. Phase Separation and Phase Mixing of Near-Critical SF_6

The liquid-vapour phase transition of two samples of SF_6 at the critical density was observed by means of a movie camera during the TEXUS-8 flight. The temperatures are recorded in the center of the fluid and on the wall of the cell. The first cell was initially in the single-phase region at a temperature $T_c + 400\,mK$ to ensure that the fluid was initially homogeneous. During the micro-*g*-period, the cell was cooled with a temperature ramp of 2.6 mK/s to $T_c - 400\,mK$ into the two-phase region. The 2nd cell was initially in the two-phase region at a temperature of $T_c - 400\,mK$ and was heated into the single-phase region to $T_c + 400\,mK$ with the same temperature ramp as the other cell [52].

The following results were obtained: both during cooling and heating, the temperature in the center of the liquid was following the wall temperature with nearly the same constant delay as in the one-*g* reference experiment. This means that temperature equilibration was not retarded under microgravity, at

Fig. 15: Density inhomogeneity in a sample of SF_6 heated from the two-phase to the one-phase region during a TEXUS flight. **(a)** $T<T_c$ **(b)** $T>T_c$

least for this rate of temperature change. During cooling it was observed that the sample uniformly assumed a yellow to brownish color. Approaching T_c it became increasingly darker and at T_c it was completely opaque. No brightening could be observed over a period of 3 minutes after crossing T_c to $T_c - 400\,\mathrm{mK}$. We interpret this observation as being the critical opalescence near T_c and the formation of a dispersion of droplets or bubbles representing the initial state of the two new phases below T_c.

In the second cell, which was heated, it was observed that the fluid was rotating in the initial stage of the experiment. This rotation was due to the spin stabilization of the rocket, damping of this flow took approximately 1 minute. The two phases could easily be discerned, due to the difference of their refractive indices, as large inhomogeneous particles.

During heating, the critical opalescence appeared at the boundary of the inhomogeneities as a dark colour (Fig. 15). The inhomogeneities could be observed up to $T_c + 400\,\mathrm{mK}$, but it can be observed that at the boundary a dissolving of the density inhomogeneities took place. The conclusion of this observation is that mixing in microgravity is a process which can take time.

A similar experiment was performed during the D-1 Mission [53]. In a later stage of the experiment, the formation of spherical droplets can be observed. The analysis of the results is still in progress.

D.2.2. Density Distribution Near the Critical Point in a Microgravity Environment

During the D-1 Spacelab Mission the density distributions in a sample of SF_6 was observed using the holographic facility "Holop" [54]. The sample was sealed in a glass capillary of 2.5 mm diameter. Initially the sample was heated up rapidly at a rate of 1.1 K/min to 2.5 K above the critical temperature. It was then cooled at a rate of 0.08 K/min and by double exposure holography, the density differences within the sample were registrated. Unexpected large density inhomogeneities were observed, they may result from the fast heating from the two-phase region, and they were not dissolved during the cooling period of 30 minutes. This result confirms the observations mentioned earlier that mass transport is very slow.

D.2.3. Phase Separation of a Critical Mixture of Isobutyric Acid and Water

This demonstration experiment was performed in a Space Shuttle in June 1985 [55] (Fig. 16a). It had been tested during the few seconds available in a parabolic aircraft flight [56] (Fig. 16b).

The isobutyric acid-water system was chosen because it meets the safety requirements for manned flight and also because its critical temperature $T_c = 30°\mathrm{C}$ can be easily reached. The isobutyric-rich phase was coloured green by traces of malachite. The experiment consisted of first, the observation of wetting layers at room temperature, where the system was in the two-phase region. Then the cell was heated by hand contact and stirred. The phase separation process could be observed by letting the temperature of the cell return to room temperature.

Very long equilibration times were observed. As expected, the wetting layers were found to be macroscopic.

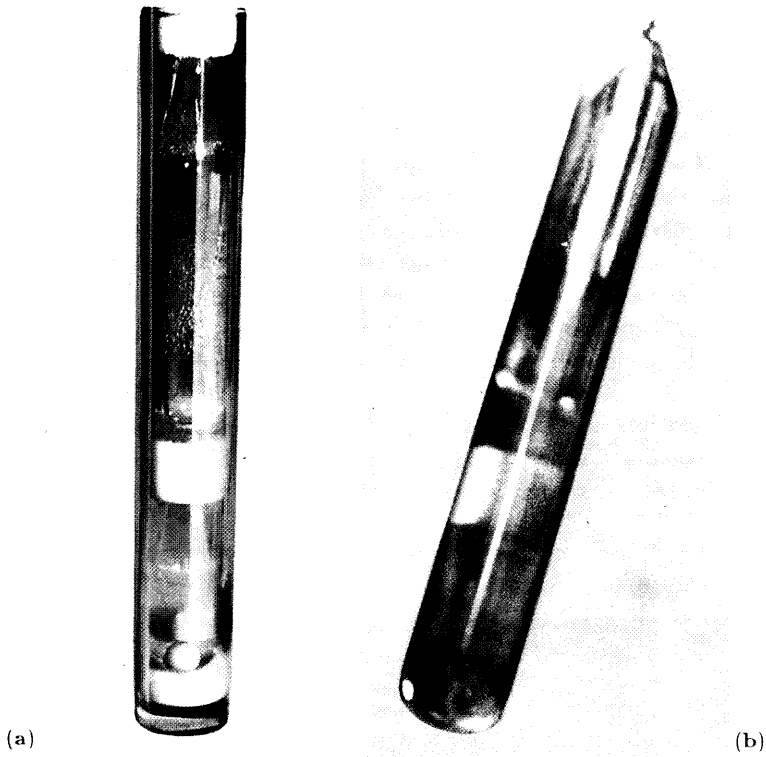

Fig. 16: **(a)** A sample of isobutyric acid and water at critical concentration in the Space Shuttle (June 1985). The acid-rich phase is coloured green and wets teflon. The aqueous phase wets glass. **(b)** Photograph taken during a parabolic flight of a similar sample, showing wetting layers. **(c)** A detailed sketch of the photograph 16 b.

D.2.4. Phase Separation of Critical and Near-Critical Mixtures of Cyclohexane-methanol and of their Deuterated Derivatives

Adding a few weight percent of deuterated cyclohexane to a binary mixture of cyclohexane and methanol allows the density of the phases to be adjusted

to be equal within 10^{-6} g cm^3, while the mixture remains a binary fluid with respect to the phase separation and critical phenomena. Moreover, the critical properties are nearly identical to those of the cyclohexane-methanol system [57].

D.2.4.1. Experiments Under One-g with Isodensity Mixtures

A study of the phase separation at the critical concentration has shown that spinodal decomposition driven by hydrodynamic instabilities occured even in the very late stages, with a linear growth of the pattern vs time $\lambda m \sim t$. Macroscopic spinodal structures have been obtained (see Fig. 17) and the final equilibrium state of the system seems governed by the wetting forces. The methanol-rich phase is wetting the container walls and surrounds the cyclohexane-rich phase.

When the concentration is only nearly critical, phase separation is not hydrodynamically governed any more, and the time to reach a final equilibrium is much increased (Fig. 18). In that case the typical droplet size increases as $\lambda m \sim t^{1/3}$.

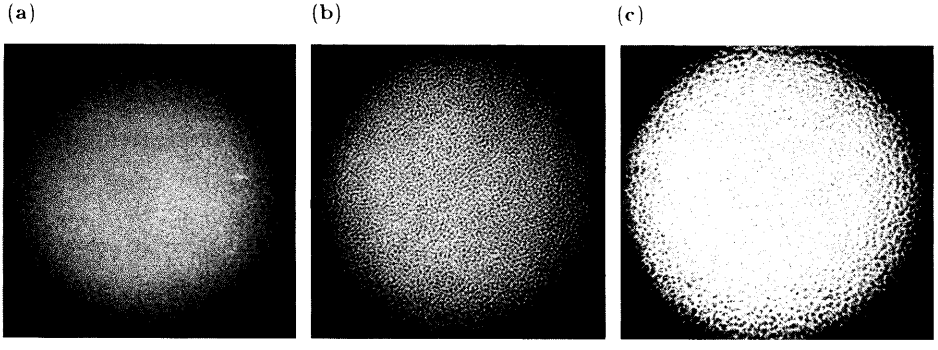

Fig. 17: Growth at the critical composition. Provided that the product $g \cdot \Delta\varrho$ remains small to avoid convection, earth and space experiments are nearly identical. The quench was 10 mK below T_c. **(a)** 30 s after the quench **(b)** 60 s after the quench **(c)** 90 s after the quench

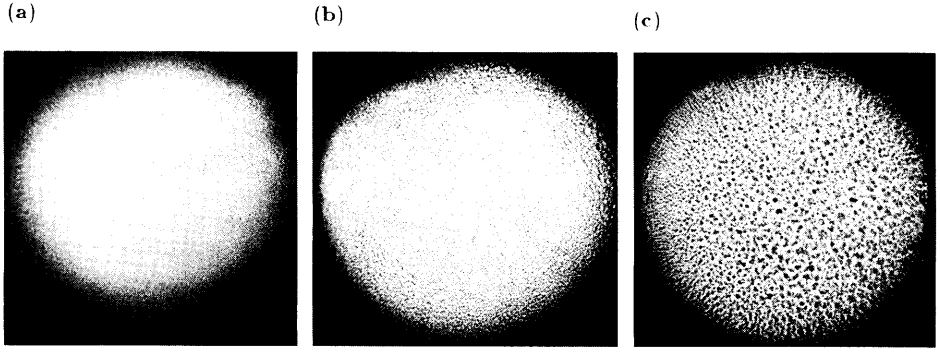

Fig. 18: Growth at near critical composition. Provided that the product $g \cdot \Delta\varrho$ remains small to avoid convection, earth and space experiments seem identical in the limit of 360 s. The quench was 10 mK below T_c. Note the difference in time scale with the Fig. 17: **(a)** 3.780 sec. after the quench **(b)** 9.600 s after the quench **(c)** 12.600 s after the quench

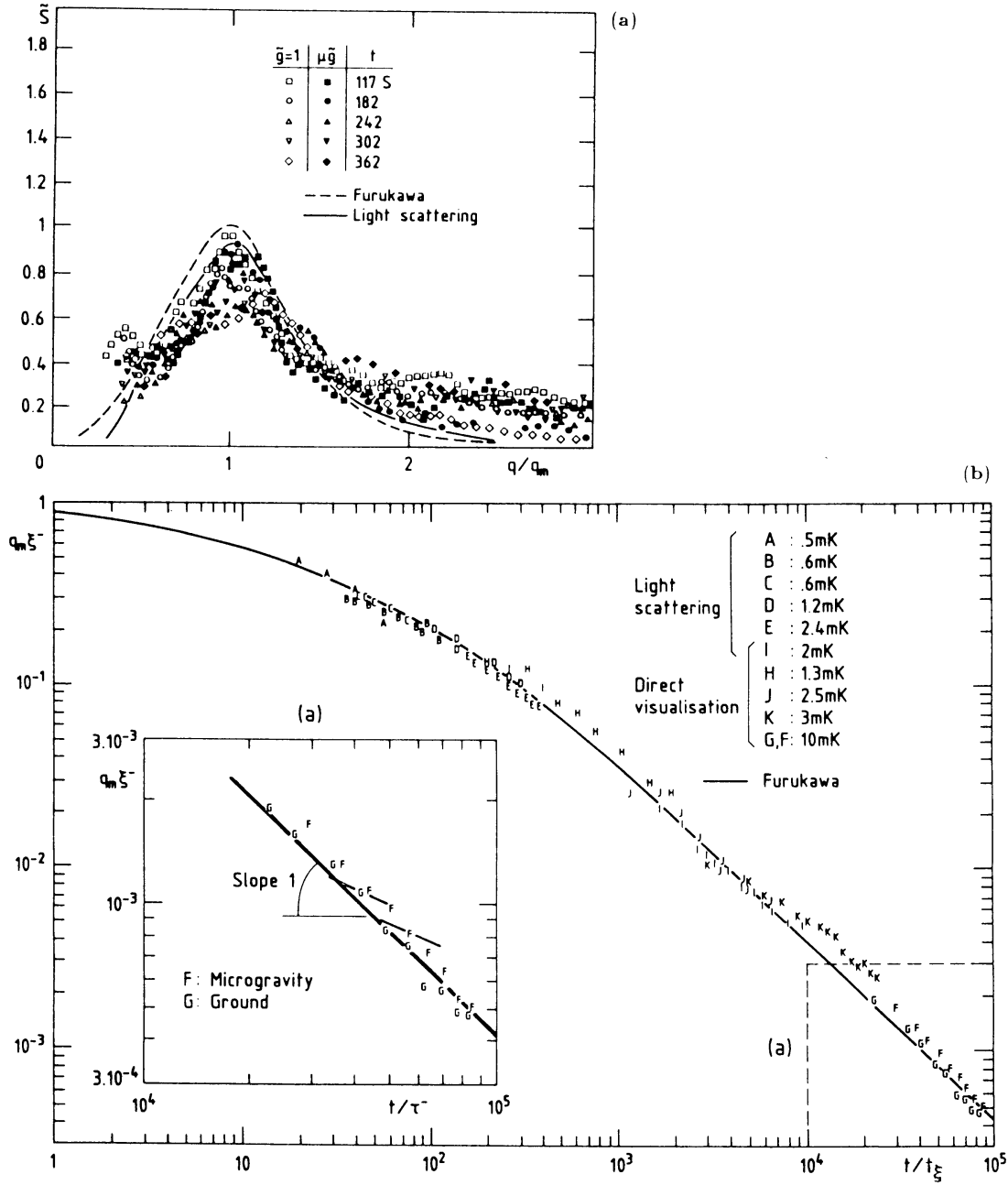

Fig. 19: **(a)** Reduced structure factors, expected to be universal, obtained from the digitization and the Fourier transforming of patterns similar to Fig. 17. Earth-based experiments in isodensity systems ($\tilde{g} = 1$) are compared to microgravity experiments (μg), light scattering data and a theoretical estimation by Furukawa. **(b)** Log-log plot of the structure wavevector $q_m = 2\pi/\lambda m$ obtained from Fig. 19 a. The quantity q_m is expressed in units of the correlation length (ξ), and the time (t) in units of the lifetime (t_ξ) associated to ξ. These results are concerned with the isodensity mixture for a quench of 10 mK below T_c. The straight line comes from theory and is expected to be universal. The bars in **(a)** correspond to 1 mK uncertainty. G: ground experiment; F: flight experiment

D.2.4.2. Microgravity experiments: Isodensity and non-isodensity mixtures

The experiments under microgravity [58] have been performed to try to answer the following question: Is an isodensity mixture a good model to predict the phase transition properties in a real space environmnent?

A preliminary analysis of a TEXUS 13 experiment (1986), where a critical isodensity mixture of cyclohexane/deuterated cyclohexane and methanol was used, has shown no major differences with the ground-based experiments (Fig. 19). This was contrary to the TEXUS 11 experiment result (1985) using a non-isodensity mixture, and where no clear phase separation could be observed during the 6 minutes duration of the experiment. However, this latter experiment suffered from a lack of precision concerning the criticality of the sample. It might have been only near-critical, within 1 %. This could have led to a much longer phase separation process, as reported in Fig. 18.

To conclude, these experiments have shown that, qualitatively and quantitatively, isodensity mixtures are indeed good models to predict – at least for short periods – the phase separation of mixtures in space, and especially at critical concentration, where the capillary character of hydrodynamics growth is definitely supported. It has also shown the dramatic influence of the volume fraction – through a deviation from criticality – on the growth processes in the critical region.

D.2.5. Phase Separation After Stirring in Aqueous Polymer Mixtures

Mixtures of polymers, such as dextran and polyethylene glycol, once mixed in aqueous solutions, can form two well defined phases at room temperature [59]. Rather than studying phase separation phenomena, interest has centered to date around their application to the partition of biological materials between the phases and the interface.

Experiments were conducted to study the coarsening rate of such mixtures after they have been homogeneized at the scale of a few microns by stirring. The observations were performed by using a photographic camera under the following conditions:

a) under a one-*g* environment with an isodensity system,
b) in an aircraft (20 s of approx. 10^{-2} g), and on board of the space shuttle.

The results have shown that both the isodensity system (on earth and in space) and the other systems generally exhibited a rapid coarsening process: the final state, governed by wetting forces, was reached after roughly 10 minutes. One sample however was not phase separated even after one hour, the interpretation of this observation is not clear at the moment.

We note that these findings seem in agreement with the above results of the phase separation experiments performed at the critical point (see above Section D.2.4.), provided that one considers the volume fraction of the phases as beeing an extra variable; this variable has been seen to be a crucial parameter to determine the coarsening rate of the growth process.

D.3. Aqueous Salt Solutions

Two preliminary experiments, using conductance techniques, have been carried out as part of the TEXUS sounding rocket program. These were designed largely to investigate the feasibility of such a study and to give an indication of the rate of equilibration to the new microgravity state of a dilute sodium chloride solution held within a few degrees of its critical point.

The experiments were identical in concept, though the second (TEXUS 12) benefitted in several ways from what was learned during and in preparation for the first (TEXUS 10). Conductance and capacitance measurements were made in a small autoclave-cell at temperatures a few K above the critical temperature of the solution.

In the TEXUS 10 flight the evidence for a gravity-induced change in resistance was obscured by the consequences of a phenomenon which occured during the heating up stage. This was a temporary, but slowly reversible, precipitation of salt as the liquid phase disappeared. Even at an average heating rate of about 1 K/h the phenomenon was observed in terrestrial experiments. Unfortunately, it was not possible to prolong the pre-launch heating period sufficiently to allow complete re-dissolution of the salt. Although there appeared to be an increase in solution resistance at microgravity, the effects of salt dissolution (accelerated in microgravity) were superimposed on this change and made it impossible to determine the rate of de-stratification.

In the TEXUS 12 experiment, a longer pre-heating period and the employment of a solution of somewhat higher mean density (and hence higher solubility) ensured the absence of solid salt at launch. On the basis of an interpolated critical temperature for the 10^{-3} m NaCl solution (374.5 ± 0.1) the strongly sedimented solution would have been at least 2 to 2.5 K above its real (zero-g) critical point. This experiment provided clear evidence for a large but fairly slow increase in solution resistance under microgravity. The 6 minutes of micro-g were not long enough to define a rate of de-stratification [60] but it appeared that the process would have taken of the order of 15 minutes for de-stratification to be half completed.

E. Prospectives

Only a few microgravity experiments on near-critical phenomena have so far been performed. Most of these have yielded unexpected results. Despite this, it is desirable to attempt to assess which areas of research should be pursued in the future. Six more or less clearly distinguishable areas are considered.

E.1. Equilibrium Thermodynamic Properties

Stratification only affects a normal fluid's thermodynamic properties very close to the critical point, where its behaviour is predictable from current theory (e.g. Renormalization Group). With binary fluid mixtures normal-g experiments al-

ready offer satisfactory verification of the theory; however, with pure fluids, there are a number of small discrepancies for some properties.

These include the critical exponents related to density and compressibility, heat capacity and correlation length. Microgravity experiments are expected to remove these discrepancies. They should also facilitate a particularly searching test of the theory's predictions concerning the λ-point of He.

Thus, at present, it appears that the main use of microgravity is to remove any remaining uncertainties there may be in the experimental verification of theory.

E.2. Approach to Equilibrium (Pure Fluids)

The approach to equilibrium on changing pressure or temperature is much better understood for binary fluid mixtures than for pure fluids. This is because of the severe buoyancy problems which, in the latter case, cannot be eliminated at normal-g. Approach to equilibrium (particularly with respect to homogenization of the two phases) is governed by quite different processes at zero and at normal-g. The critical anomalies in the fluid's transport properties (see Section E.3.) are clearly of direct relevance, but neither the normal nor the zero-g processes are well understood.

It is particularly important to understand well the processes which control the approach to equilibrium at zero-g because they will influence all future zero-g measurements of more fundamental properties.

E.3. Transport Properties

Potentially relevant properties are viscosity, thermal conductivity, thermal diffusivity and decay of the order parameter (optical light scattering). Effects additional to stratification are involved and a number of specific areas require attention. Of principal interest is thermal diffusivity because of the extreme sensitivity to convection (the Rayleigh number diverges at the critical point). As with the thermodynamic properties (see Section E.1.), it currently looks as if a relatively small number of experiments should be able to tidy up all the outstanding uncertainties in the various critical exponents. Completion of this task is likely to take longer than for already fairly well-defined static exponents but it should eventually be possible to complete the task of reconciling theory and experiment.

E.4. Phase Separation Processes

There is currently an imperfect understanding of the processes which lead to the growth of the separated bulk phases under both normal and zero-g. An improved understanding of these processes is required in connection with several technically important areas of metallurgy. The removal of gravity-induced instabilities (e.g. convection) under microgravity has already yielded some advances in understanding. Inevitably (as with the processes referred to in E.3.), future research appears to be more open-ended than that directed towards the verification of critical exponents.

E.5. Interfacial Phenomena

Microgravity should be able to help in understanding both the formation of interfaces and the behaviour of capillary waves.

There are a number of theoretical problems and areas where the situation is unclear – especially under conditions of near zero-g. The g-dependence of these processes at low g could very usefully be investigated.

E.6. Electrolyte Solutions

In this area the influence of g on the equilibrium state is large – so large that a really systematic study (theoretical and experimental) of the physical chemistry of electrolyte solutions in compressible solvents has been severely inhibited. Studies under non-stratified zero-g conditions are needed to test appropriate theories as they are developed. In addition, a systematic study of the influence of g between 0 and 1 g will be needed so that the relationship between the solution structure at normal and at zero-g can be established and normal g experiments can be reliably interpreted. There is much to be done before this goal is reached.

F. References

1. van der Waals J.D., "Over de Continuiteit van den Gas en Vloeistoftoestand", Thesis Univ. of Leiden, 1873
2. Andrews T., "On the continuity of the gaseous and liquid state of matter", Phil. Trans. R. Soc. **159** (1869), 575
3. van der Waals J.D., "Die Continuität des gasförmigen und flüssigen Zustandes", Part 1, J.A. Barth, Leipzig, 1900
4. Gouy M., "Effets de la pression sur les fluides au point critique", C.R. Acad. Sci. (Paris), **115** (1892), 720
5. Landau L. and Lifshitz E., see "Statistical Physics" – MIR Moscow 1967
6. See e.g. Kumar A., Krishnamurty H.R. and Gopal E.S.R., "Equilibrium Critical Phenomena in Binary Liquid Mixtures", Phys. Rep. **98** (1983), 57
7. Moldover M.R., Hocken R.J., Gammon R.W., Sengers J.V., "Overviews and Justifications for Low Gravity Experiments on Phase Transition and Critical Phenomena in Fluids", NBS Techn. Note 925, 1976
   Moldover M.R., Sengers J.V., Gammon R.W., Hocken R.J., "Gravity effects in fluids near the gas-liquid critical point", Reviews of Modern Physics, Vol. **51** n° (1979), 79
8. Corwin J.F., Bayless R.G. and Owen G.E., "The conductivity of dilute sodium chloride solutions under supercritical conditions", J. Phys. Chem. **64** (1960), 641
9. Turner D.J., "Electrolyte solutions near the critical point of water", Proc. 4th European Symposium on Materials Sciences under Microgravity, Madrid (1983), ESA-SP-191, p. 393
10. Ma S.K., "Modern Theory of Critical Phenomena", Benjamin, Massachusetts, 1976
11. Pfeuty P. and Toulouse G., "Introduction to the Renormalization Group and Critical Phenomena, Wiley, New York, 1977
12. Amit D.J., "Field Theory, the Renormalization Group, and Critical Phenomena", McGraw-Hill, New York, 1978
13. Hohenberg P.C., "Microscopic Structure and Dynamics of Liquids", Ed. J. Dupuy and A.J. Dianoux (Plenum), New York, 1978
14. Sengers J.V. and Levelt Sengers J.M.H., "Progress in Liquid Physics", Ed. C.A. Croxton (Wiley, Chichester), 1978
15. Wilson K., "Problems of Physics with many scales of length", Sci. LAm. **241** (1979), 140

16. Reichl L.E., "A modern course in Statistical Physics", Univ. Texas Press, Austin, 1980
17. Rowlinson J.S. and Swinton F.L., "Liquids and Liquid Mixtures", 3rd Ed. (Butterworths), London, 1982
18. Moldover M.R., in "Phase Transitions", Cargese 1980, Ed. M. Levy, J.C. Le Guillou, J. Zinn-Justin (Plenum), New York, 1982
19. Sengers J.V., in "Phase Transitions", Cargese 1980, Ed. M. Levy, J.C. Le Guillou, J. Zinn-Justin (Plenum), New York, 1982
20. Stanley H.E., "Introduction to Phase Transitions and Critical Phenomena", Oxford Univ. Press, New York, 1971
21. Beysens D., in "Phase Transitions", Cargese 1980, Ed. M. Levy, J.C. Le Guillou, J. Zinn-Justin (Plenum), New York, 1982, 25–62
Beysens D., in "Material Sciences in Space", Ed. Feuerbacher B., Hamacher H. and Naumann B., Springer Berlin (1986), 191
22. Beysens D., "Critical Point Phenomena in Fluids", Proc. 4th European Symposium on Materials Science under Microgravity, Madrid (1983), ESA-SP-191, 367-376
23. Huijser P.H., Michels A.C. and Trappeniem N.J., "Optical Investigation of Critical Behaviour in Simple Fluids at Reduced Gravity", Proc. 4th European Symposium on Materials Science under Microgravity", Madrid (1983), ESA-SP-191, 377–393
24. Findenegg Q.H., "Adsorption behaviour of pure fluids near the gas-liquid critical point", Proc. 4th European Symposium on Materials Science under Microgravity, Madrid (1983), ESA-SP-191, 385–391
25. Straub J. and Schiebener P., to appear
26. Sengers J.V., van Leeuwen J.M.J. "Gravity effects on critical fluctuations in gases", J. Phys. Chem. **88** (1984), 6479
27. van Leeuwen J.M.J., Sengers J.V., "Gravity effects on the correlation length in gases near the critical point", Physica 128A, **131** (1984), 99
28. Wilson K.G. and Kogut J.B., Phys. Rev. **12** (1974), 75
29. See e.g. Sengers J.V., "Transport properties of fluids near critical points", Int. J. of Thermodyn. **6** (1985), 203 and ref. therein
30. Kawasaki K., in "Phase transitions and critical phenomena", Ed. C. Domb and M.S. Green, Academic Press, New York, 1976
31. Jany P. and Straub J., "Thermal diffusivity of fluids in a broad region around the critical point", Int. J. of Thermophysics, Vol.8, 165-180 (1987)
32. See e.g. Beysens D., Gbadamassi M. and Moncef-Bouanz, "New developments of binary fluids under shear flow", Phys. Rev. **A28** (1983), 2491 and ref. therein
Onuki A., Yamasaki K. and Kawasaki K., "Light scattering by critical fluids under shear flow", Ann. Phys. N.Y. **131** (1981), 217
33. Cahn J.W., "Spinodal Decomposition", Trans. Metall. Soc. AIME **242** (1968), 166
34. See e.g. Gunton J.D., San-Miguel M. and Sahni P. in "Phase transitions and critical phenomena", vol. 8, Ed. C. Domb and J.L. Lebowitz (Academic, New York), 1983
35. Siggia E.D., "Late stages of spinodal decomposition in binary mixtures", Phys. Rev. **A20** (1979), 595
36. Cahn J.W., "Critical point wetting", J. Chem. Phys. **66** (1977), 3667 For a review, see e.g. "Fundamental problems in statistical mechanics VI", Ed. E.G.D. Cohen (Elsevier, Amsterdam), 1985
37. See e.g. Moldover M.R. and Schmidt J.W., "Wetting, multilayer-adsorption, and interfaces phase transitions", Physica **351** (1984)
38. Beaglehole D., "Adsorption and wetting at the liquid-vapour interface of cyclohexane-methanol-water mixtures", J. Phys. Chem. **87** (1983), 4749
39. Fisher M.E. and de Gennes P.G., "Phénomènes aux parois dans un mélange binaire critique", C.R. Acad. Sci. Paris **287B** (1978), 207
Beysens D. and Leibler S., "Observation of an anomalous adsorption in a critical binary fluid", J. Phys. Lettres, Paris-43, L-133 (1982)
Franck C. and Schnatterly S.E., "New critical anomaly induced in a binary liquid mixture by a selectively adsorbing wall", Phys. Rev. Lett. **48** (1982), 763
40. Lipa J.A., "Lambda transition flight program" in "Microgravity science and applications", Report on workshop 3–4 Dec. 1984, National Academic Press, Washington D.C. (1986), p. 265
41. Turner D.J., "Thermodynamics of high-temperature aqueous systems" in "Thermodynamics of aqueous systems with industrial applications", Ed. S.A. Newman, 1980, ACS Symposium series n° 133, p. 653

42. Wood R.H., Quint J.R., Grolier J-P.E., "Thermodynamics of a charged hard sphere in a compressible dielectric fluid", J. Phys. Chem. **85**, 1981, 3944
43. Gates J.A., Wood R.H. and Quint J.R., "Experimental evidence for the remarkable behaviour of the partial molar heat capacity at infinite dilution of aqueous electrolytes at the critical point", J. Phys. Chem. **86** (1982), 4948
44. See e.g. Ramakrishnan J., Nagarajan N., Kumar A., Gopal E.S.R., Chandrasekhar P. and Ananthakrishna, "Critical behaviour of electrical resistivity in polar and non-polar binary liquid mixtures", J. Chem. Phys. **68** (1978), 4098
45. Straub J., "Dichtemessungen am kritische Punkt", Thesis, Technische Universität München (1966), Habilitation Technische Universität, München (1977)
Straub J., "Kritische Phänomene in reinen Fluiden", 18. Bunsen-Kolloquium, 15 Nov. 1983, Ed. J. Richter, Aachen
46. Sengers J.V., Moldover M.R., "Critical phenomena in space?" Z. Flugwiss. Weltraumforsch. 2 (1978), Heft 6, 371
47. Robert M., "Absence of phase separation for fluids in three dimensions", Phys. Rev. Lett. **54** (1985), 444
48. Chatterjee S., Vani V., Guha S. and Gopal E.S.R., "Critical wetting phenomena: observation of hydrodynamic instabilities", J. Phys. Paris **46** (1985), 1533
49. Nitsche K., Straub J. and Lange R., "Isochoric specific heat of sulfur hexafluoride at the critical point – A Spacelab experiment for the German D-1 mission in 1985", Proc. 5th European Symposium on Materials Science under Microgravity, Elmau (1984), ESA-SP-222, 335
50. Straub J., Lange R., Nitsche K. and Kemmerle K., "Isochoric specific heat of SF_6 at the critical point: Laboratory results and outline of a Spacelab experiment for the D-1 mission in 1985", Int. J. Thermophysics **7** (1986), 343–356
51. Nitsche K., Straub J., "The isochoric specific heat of sulfur hexafluoride SF_6 at the critical point under microgravity conditions", Proc. of the Symposium of the D-1 mission, Norderney, to be published
Nitsche K., Straub J., The critical "Hump" of Cv under microgravity – Results from the D-1 Spacelab experiment "Wärmekapazität", Proc. of the 6th European Symposium on Materials Science under Microgravity, Bordeaux (1986), ESA-SP-256, 109
Nitsche K., Straub J., "Die isochore Wärmekapazität am kritischen Punkt unter reduzierter Schwerkraft", Naturwiss. **73** (1986), 370–373
52. Nitsche K., Straub J., Lange R., "Ergebnisse des TEXUS 8 Experiments "Phasenumwandlung" – Forschungsbericht Luft und Raumfahrt BMFT (1984) – In preparation for publication
53. Messerschmidt E. and Straub J., Private communication (1985)
54. Klein H. and Wanders K., "Density distribution near gas/liquid critical point under reduced gravity", Naturwiss. **73** (1986), 374–375
Klein H., Wanders K. and Neuhaus D., "Holografic experiments: Results of Spacelab D-1", Proc. of the 6th European Symposium on Materials Science under Microgravity, Bordeaux (1986), ESA-SP-256, 105
55. Baudry P. and Beysens D., private communication (1985)
56. Legros J.C. and Beysens D., private communication (1984)
57. Houessou C., Guenoun P., Gastaud R., Perrot F. and Beysens D., "Critical behaviour of the binary fluids cyclohexane-methanol, deuterated cyclohenaxe-methanol and of their isodensity mixture: Application to microgravity simulations and wetting phenomena", Phys. Rev. A32 (1985), 1818
58. Beysens D., Guenoun P. and Perrot F., "Phase separation of critical binary fluids under microgravity: Comparison with isodensity conditions", submitted to Phys. Rev. A
Perrot F., Guenoun P. and Beysens D., "Physicochemical hydrodynamics: Interfacial phenomena", Ed. M.G. Velarde and B. Nichols (Plenum, 1986) – in press
Beysens D., Guenoun P. and Perrot F., "Phase separation in microgravity of binary fluids near a critical point", Proc. of the 6th European Symposium of Materials Science under Microgravity, Bordeaux (1986), ESA-SP-256, 139
59. van Alstine J.M., Harris J.M., Snyder S., Curreri P.A., Bamberger S., Brooks D.E., "Separation of aqueous two-phase polymer systems in microgravity", Proc. of the 5th European Symposium on Materials Science under Microgravity, Elmau (1984), ESA-SP-222, 309

Curreri P.A., van Alstine J.M., Brooks D.E., Bamberger S., Snyder R.S., "On the stability of high volume fraction immiscible dispersions in low gravity", submitted to Metall. Trans. A

60. Turner D.J., "Electrolyte solutions near the critical point of water," Proc. of the 6th European Symposium on Materials Science under Microgravity, Bordeaux (1986), ESA-SP-256, 125. Also paper in preparation for J. Chem. Sor. Faraday Trans.